Supporting information

Luminescent coordination polymeric gels based on rigid terpyridyl phosphine and Ag(I)

Xin Tan, Xue Chen, Jianyong Zhang,* and Cheng-Yong Su

KLGHEI of Environment and Energy Chemistry, School of Chemistry and Chemical Engineering, Sun Yat-Sen University, Guangzhou, 510275, China. E-mail: zhjyong@mail.sysu.edu.cn

Experimental

Synthesis of 4'-(4-fluorophenyl)-4,2':6',4"-terpyridine (**Py2F**): 4-Acetylpyridine (0.06 mol，7.2684 g) was added to a solution of 4-fluorobenzaldehyde (0.03 mol，3.7233 g) in EtOH (200 mL). KOH pellets (0.06 mol, 4.1056 g) were then added followed by aqueous NH_3 (25%, 5.6 mL, 0.075 mol). The resulting reaction mixture was stirred at RT for 24 h, during which time a white suspension formed. The solid was collected by filtration, washed with EtOH and recrystallised with $CHCl_3$-MeOH, affording a white crystalline product (yield 4.52 g, 46%). ^{1}H NMR (300 MHz, $CDCl_3$): δ/ppm 8.75 (d, $^3J_{H\text{-}H}$ = 4.7 Hz, 4H), 8.04 (d, $^3J_{H\text{-}H}$ = 4.7 Hz, 4H), 7.95 (s, 2H), 7.69 (t, $^3J_{H\text{-}F}$ = 7.5 Hz, 2H), 7.22 (d, $^3J_{H\text{-}H}$ = 7.6 Hz, 2H). ^{19}F NMR (282 MHz, $CDCl_3$): δ/ppm -111.8.

Synthesis of 4'-(4-diphenylphosphinophenyl)-4,2':6',4"-terpyridine (**Py2Phos**): The reaction was performed under pure dry nitrogen using standard Schlenk techniques. To **Py2F** (1.6368 g, 5 mmol) in THF (100 mL, distilled from potassium under nitrogen prior to use) was added dropwise $KPPh_2$ (10 mL, 0.5 mol L^{-1}, 5 mmol) with stirring. The reaction mixture was brought to reflux for 24 h. THF was removed under reduced pressure and MeOH (10 mL) was added to the residue. The white solid was collected by filtration and washed with MeOH (10 mL × 3). Yield: 1.80 g, 73%. ^{1}H NMR (300 MHz, $CDCl_3$): δ/ppm 8.78 (d, $^3J_{H\text{-}H}$ = 6.1 Hz, 4H), 8.07 (d, $^3J_{H\text{-}H}$ = 6.1 Hz, 4H), 8.03 (s, 2H), 7.72 (d, $^3J_{H\text{-}H}$ = 7.1 Hz, 2H), 7.47 (d, $^3J_{H\text{-}P}$ = 7.4 Hz, 2H), 7.37 (m, 10H). ^{31}P NMR (121.5 MHz, $CDCl_3$): δ/ppm 4.5. IR (KBr, cm^{-1}): 1592vs, 1556m, 1530w, 1492w, 1475w, 1433m, 1398w, 1386m, 1065w, 995w, 849w, 823s, 747s, 698s, 643s, 628m, 502w. **Py2Phos** is soluble in $CHCl_3$, DMF, THF and dioxane, and is slightly soluble in toluene.

Synthesis of gel: Typical procedure: A solution of **Py2Phos** (9.6 mg, 0.0195 mmol) in $CHCl_3$ (1 mL) and an AgOTf solution (5.0 mg, 0.0195 mmol) in MeCN (1 mL) were mixed and stirred protected from light for 5 min. After standing for 3 h at RT, a clear transparent gel formed.

Synthesis of Ag(**Py2Phos**)$_2$OTf·xH$_2$O (**Ag-OTf**): A solution of **Py2Phos** (5.6 mg, 0.01 mmol) in $CHCl_3$ (4 mL) was added to an AgOTf solution (2.6 mg, 0.01 mmol) in MeCN (4 mL). The reaction mixture was stirred protected from light for 5 min, and then heated in a closed container at 50 ^{o}C for 72 h. Colourless block crystals were obtained (3.5 mg, yield 50% based on **Py2Phos**). Microanalysis: found (calc.) for $C_{67}H_{48}AgF_3N_6O_3P_2S·3.5H_2O$: C 61.22 (61.60); H 3.804 (4.256); N 6.367 (6.436)%. IR (nujol, cm^{-1}): 1595m, 1531w, 1265s, 1215w, 1146m, 1092w, 1064w, 1025m, 996w, 821s, 745s, 695m, 629m, 532w, 498m.

Synthesis of Ag(**Py2Phos**)$_2$BF$_4$·H$_2$O (**Ag-BF$_4$**): A solution of **Py2Phos** (12.7 mg, 0.0257 mmol) in $CHCl_3$ (3 mL) was added to an $AgBF_4$ solution (2.5 mg, 0.0128 mmol) in MeCN (3 mL). The reaction mixture was stirred protected from light for 5 min, and then heated in a closed container at 80 ^{o}C for 24 h. Colourless block crystals were obtained (9.5 mg, yield 63 % based on **Py2Phos**). Microanalysis: found (calc.) for $C_{66}H_{48}AgBF_4N_6P_2·H_2O$: C 65.67 (66.10); H 4.226 (4.214); N 7.115 (7.010)%.

Characterisation: Scanning electron micrographs were recorded on a JSM-6330F Field Emission Scanning Electron Microscope. The samples were prepared by dispersing the gel in EtOH and placing on top of conductive glass stubs, and drying at RT followed by drying in vacuum. Prior to examination the xerogels were coated with a thin layer of gold. Transmission electron micrographs were recorded on a JEOL JEM-2010HR microscope. The samples for TEM were prepared by dispersing the aerogels in $CHCl_3$-EtOH with sonication, and carbon-coated copper grids were placed in for three times. FT-IR spectra of the aerogels were taken in a KBr disc with nujol on a Nicolet/Nexus-670 FT-IR spectrometer in the range of 4000-450 cm^{-1}. X-ray photoelectron spectroscopy was measured on a Thermo-VG Scientific ESCALAB 250 spectrometer under the pressure ~2 × 10^{-9} mbar fitted with X-ray monochromatised Al Kα radiation (15 kV 150 W, spot

size = 500 μm). Powder X-ray diffraction patterns of the samples were measured on a Rigaku D/MAX 2250 V diffractometer using monochromatized CuKα (λ = 0.15418 nm) radiation under 40 kV and 100 mA.

X-ray crystallography: Single-crystal X-ray diffraction data were collected on an Oxford Germini S Ultra diffractometer with Cu Kα radiation (λ = 1.54178 Å) for **Ag-OTf** at 150 K and for **Ag-BF$_4$** at 298 K. Both the structures were solved by the direct methods following difference Fourier syntheses and refined by the full-matrix least-squares method on F^2 using the SHELXL-97 software.[1] The non-hydrogen atoms were refined anisotropically, while the hydrogen atoms were introduced in calculated positions and refined by using a riding model. For **Ag-BF$_4$**, the solvated water hydrogen atoms were not located. The OTf$^-$ and BF_4^- anions were crystallographically disordered over two twofold-axis-related positions with 0.5/0.5 occupancy for **Ag-OTf** and **Ag-BF$_4$**, respectively. For **Ag-OTf**, proper restraints were applied to model the OTf$^-$ anion in normal geometry. For **Ag-BF$_4$**, the F atoms were refined isotropically, and appropriate restraints were applied to the large differences in the anisotropic displacement parameters along Ag-P bond.

Crystal data for **Ag-OTf**: $C_{67}H_{48}AgF_3N_6O_3P_2S$, M = 1243.98, monoclinic, space group *C2/c*, a = 10.0247(2), b = 28.8156(4), c = 20.0865(4) Å, V = 5647.13(18) Å^3, Z = 4, T = 150(2) K, ρ_{calcd} = 1.463 g cm^{-3}, μ = 4.280 mm^{-1}, F(000) = 2544, 16501 reflections were collected with 4494 unique for 3.07 < θ < 62.51, R_{int} = 0.0393, R_1 = 0.0278, wR_2 = 0.0676 ($I > 2\sigma(I)$), R_1 = 0.0313, wR_2 = 0.0711 (all data) for 404 parameters, GOF = 1.055. CCDC 854926.

Crystal data for **Ag-BF$_4$**:$C_{66}H_{48}AgBF_4N_6O_2P_2$, M = 1213.72, monoclinic, space group *C2/c*, a = 10.2064(2), b = 28.9067(4), c = 20.2929(5) Å, V = 5761.9(2) Å^3, Z = 4, T = 298(2) K, ρ_{calcd} = 1.399 g cm^{-3}, μ = 3.860 mm^{-1}, F(000) = 2480, 8220 reflections were collected with 4465 unique for 3.80 < θ < 62.53, R_{int} = 0.0323, R_1 = 0.0459, wR_2 = 0.1201 ($I > 2\sigma(I)$), R_1 = 0.0523, wR_2 = 0.1273 (all data) for 367 parameters, GOF = 1.024. CCDC 854927.

(1) G. M. Sheldrick, *SHELXL 97, Program for Crystal Structure Solution and Refinement*, Göttingen University, Germany, 1997.

Table S1 Gelation tests of **Py2Phos** and AgOTf (L:Ag = 1:1) in different solvents (0.025 mmol of **Py2Phos** and 0.025 mmol of AgOTf were dissolved in each 1 mL of solvent, and mixed).

Py2Phos	AgOTf	Result
$CHCl_3$	CH_3CN	Transparent to opaque gel after 30 min
$CHCl_3$	DMF	Transparent gel after 18 h
THF	CH_3CN	White precipitate (if diluted to 0.0072 mmol L^{-1}, transparent gel formed after 2 h)
THF	DMF	Transparent gel after 2 d
$CHCl_3$	CH_3OH	White precipitate
THF	THF	White precipitate
DMF	DMF	Solution, and colourless crystals formed after 5 h
DMF	CH_3CN	Solution, and colourless crystals formed after 4 h
DMF	CH_3NO_2	Weak gel after 24 h with colourless crystals
Toluene	CH_3CN	White precipitate
Dioxane	CH_3CN	White suspension

Table S2 Response of the gel towards various anions (0.0125 mmol of salt in 0.5 mL of $CHCl_3$ was topped on 0.0125 mmol of the gel, and standing at RT).

Salt	Result
$[Bu_4N][OTf]$	No immediate change, and crystals formed standing for overnight
$[Me_4N][NO_3]$	No immediate change, and crystals formed standing for overnight
$[Bu_4N][PF_6]$	No immediate change, and crystals formed after standing for 2 d
$[Bu_4N][BF_4]$	No immediate change, and crystals formed after standing for 2 d
$[Bu_4N][ClO_4]$	No immediate change, and crystals formed after standing for 2 d
$[Bu_4N]Br$	Dissolved immediately to form clear solution, and crystals formed after standing for overnight
$[Bu_4N]Cl$	Dissolved immediately to form clear solution, and crystals formed after standing for overnight
$[Bu_4N]OAc$	Dissolved immediately, and crystals formed after standing for 2 d

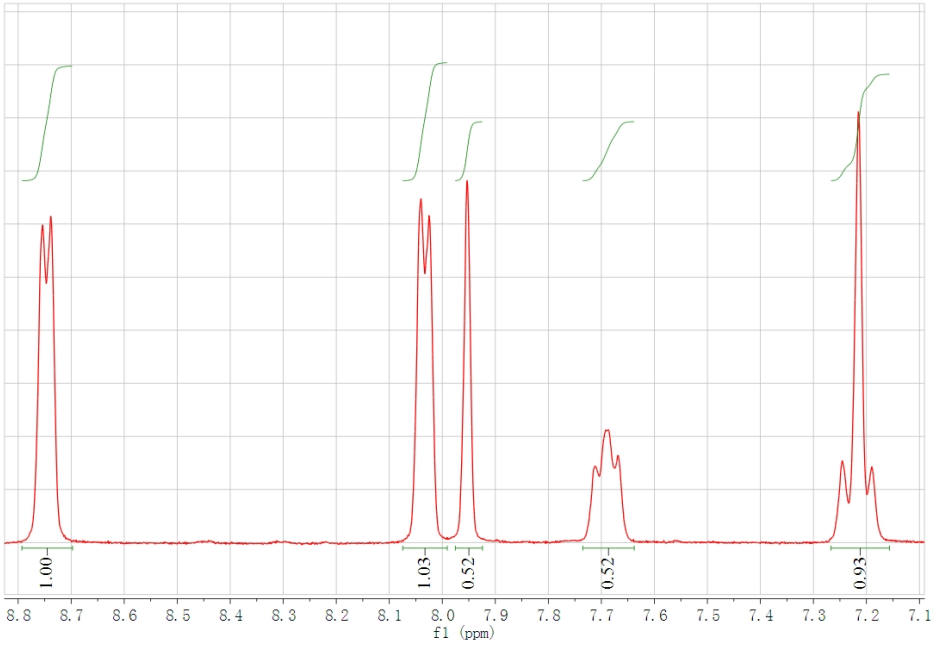

Fig. S1 ^{1}H NMR (300 MHz) of **Py2F** in $CDCl_3$ at 300 K.

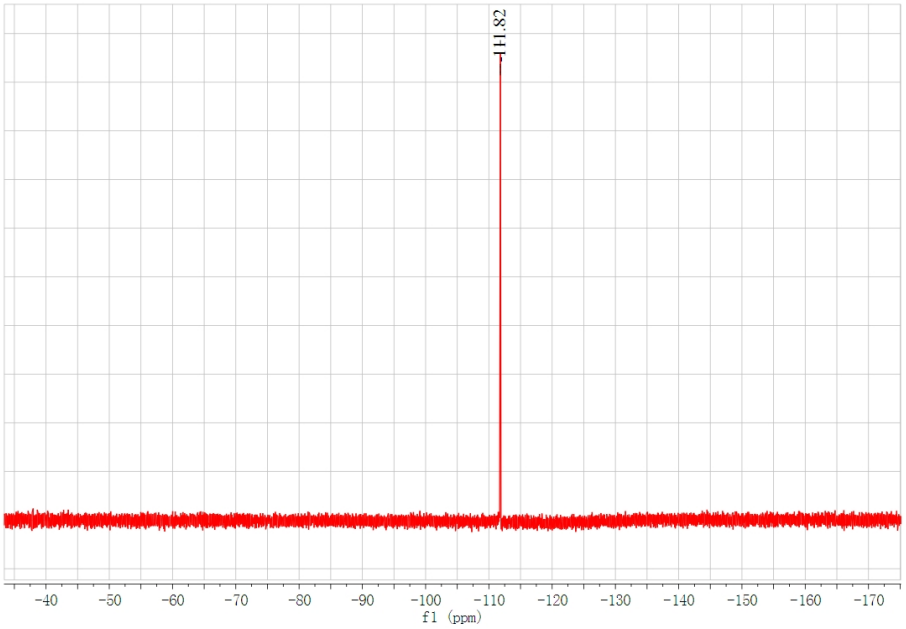

Fig. S2 ^{19}F NMR (282.3 MHz) of **Py2F** in $CDCl_3$ at 300 K.

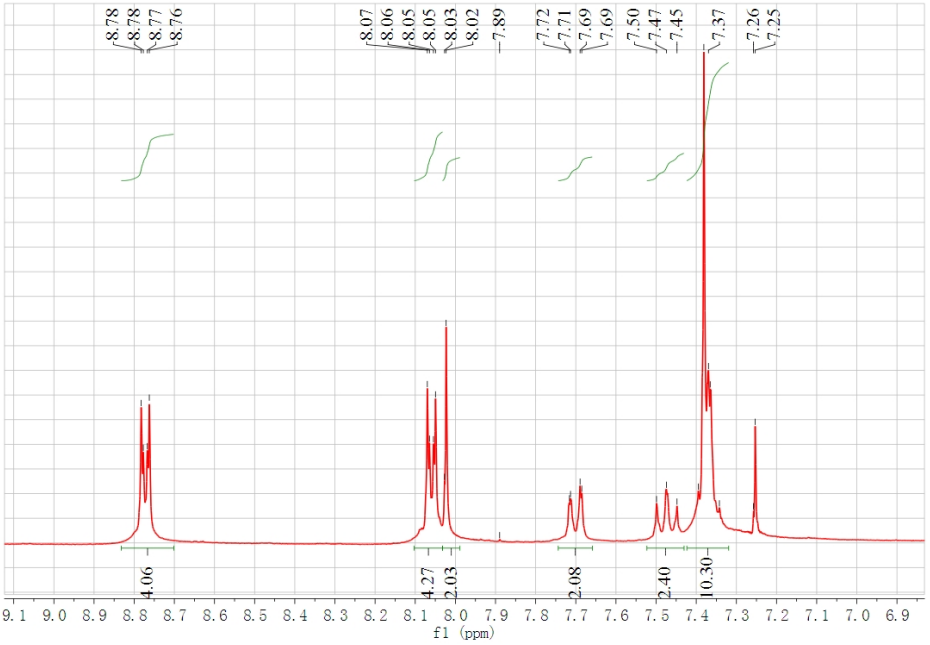

Fig. S3 ^{1}H NMR (300 MHz) of **Py2Phos** in $CDCl_3$ at 300 K.

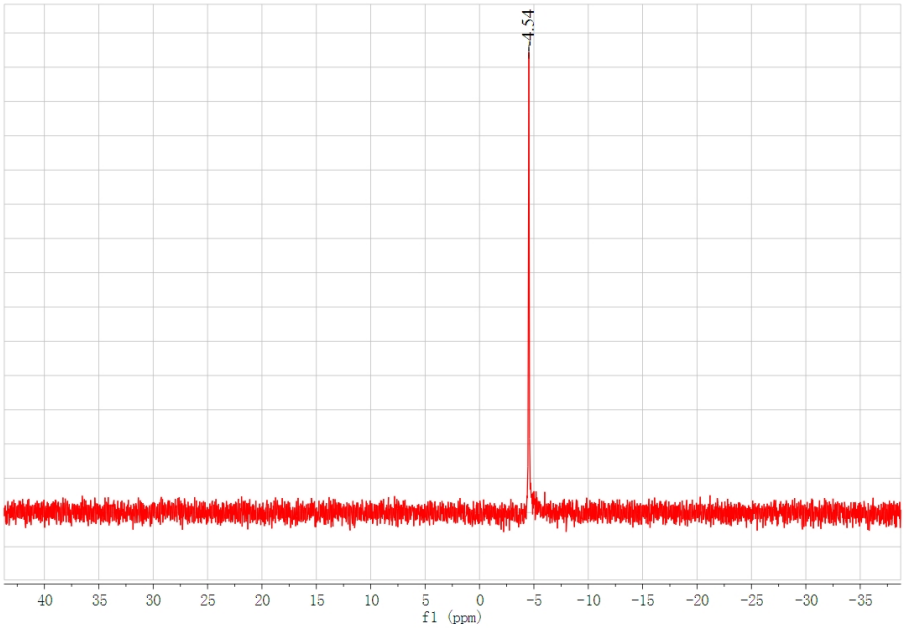

Fig. S4 $^{31}P\{^{1}H\}$ NMR (121.5 MHz) of **Py2Phos** in $CDCl_3$ at 300 K.

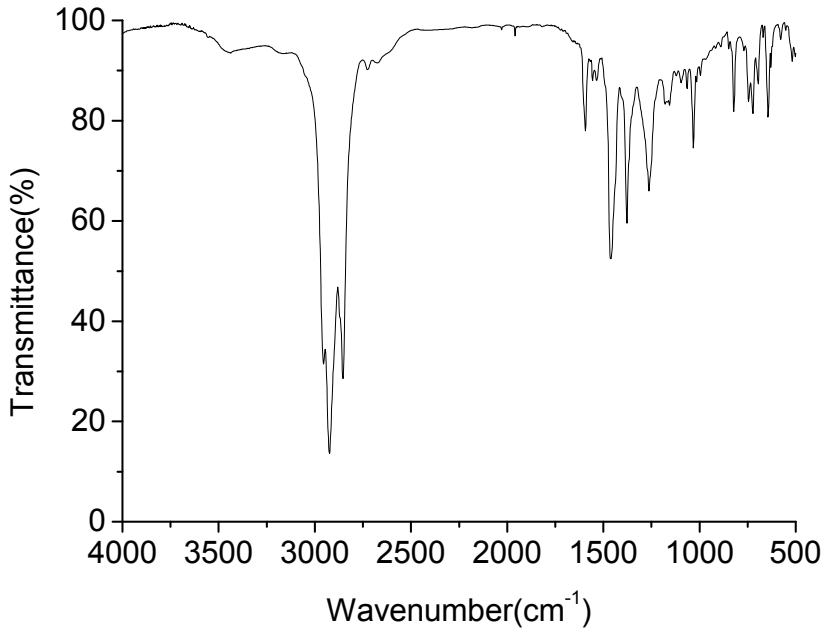

Fig. S5 FT-IR spectrum (KBr) of **Py2Phos**.

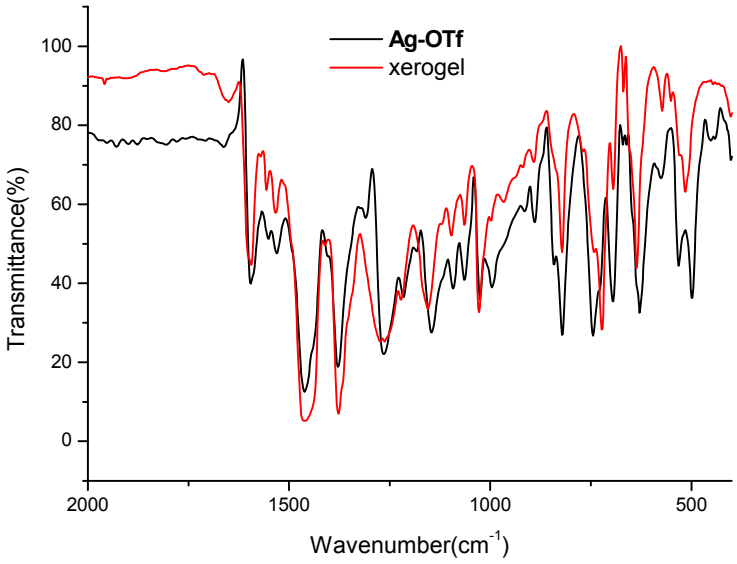

Fig. S6 FT-IR spectra of **Ag-OTf** and the AgOTf/**Py2Phos** = 1:1 xerogel in nujol.

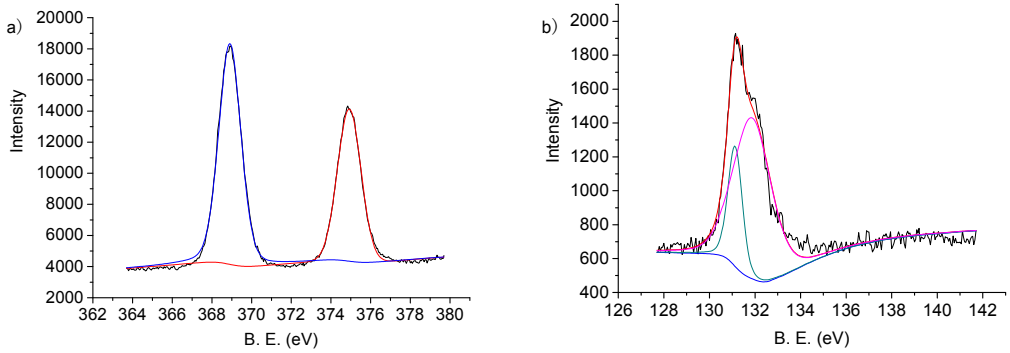

Fig. S7 XPS Ag 3d (a) and P 2p (b) spectra and the deconvoluted spectra for the xerogel.

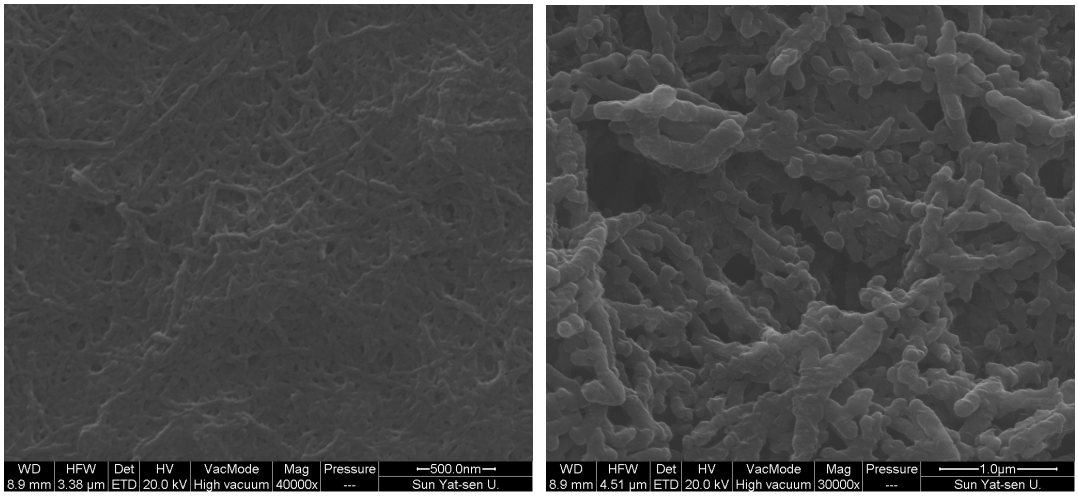

Fig. S8 SEM images of the $CHCl_3$-MeCN xerogel.

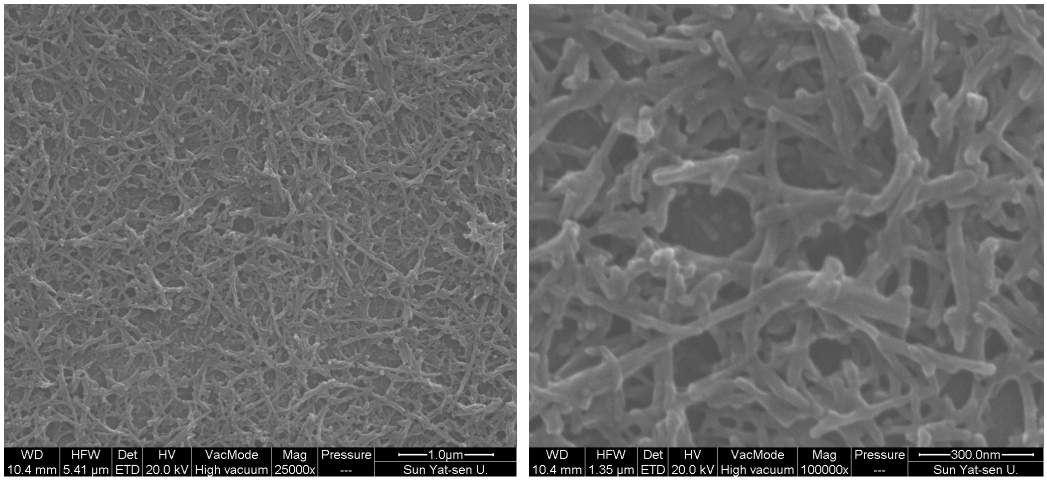

Fig. S9 SEM images of the $CHCl_3$-MeCN xerogel after solvent exchange with toluene.

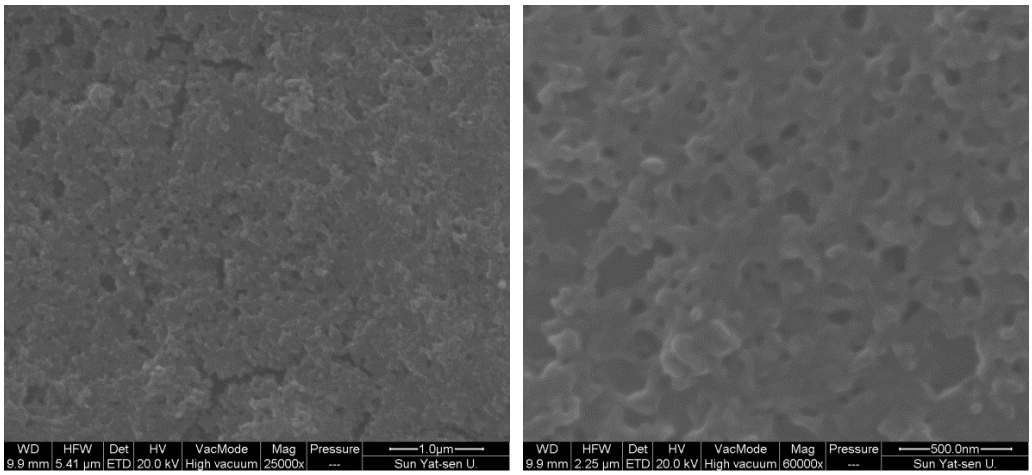

Fig. S10 SEM images of the THF-DMF xerogel.

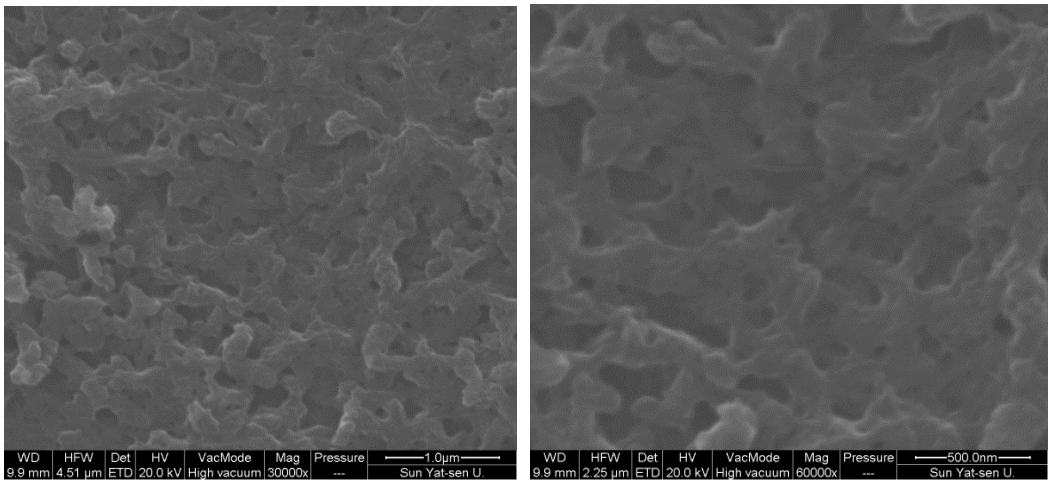

Fig. S11 SEM images of the $CHCl_3$-DMF xerogel.

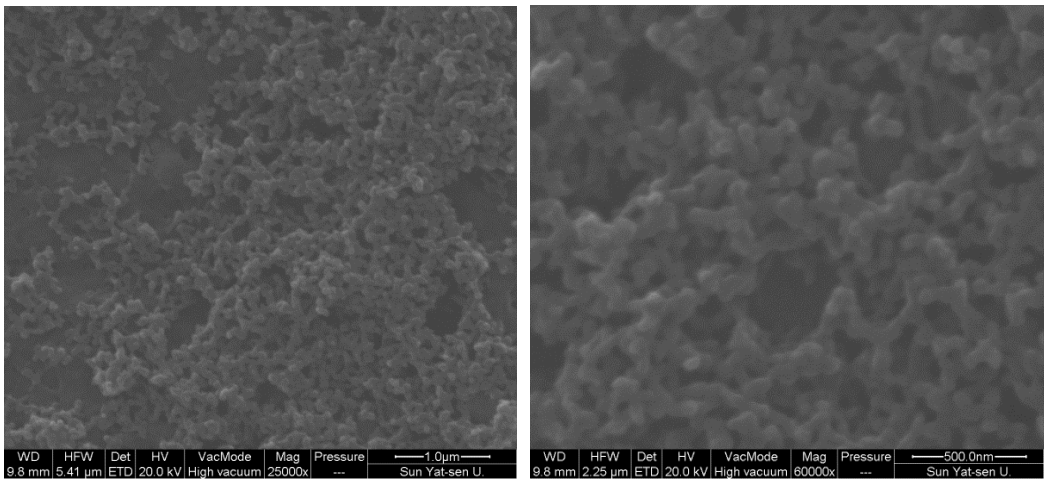

Fig. S12 SEM images of the THF-MeCN xerogel.

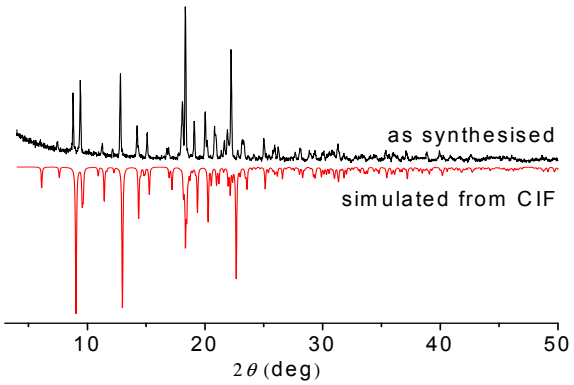

Fig. S13 Simulated and measured powder XRD patterns of **Ag-OTf**.

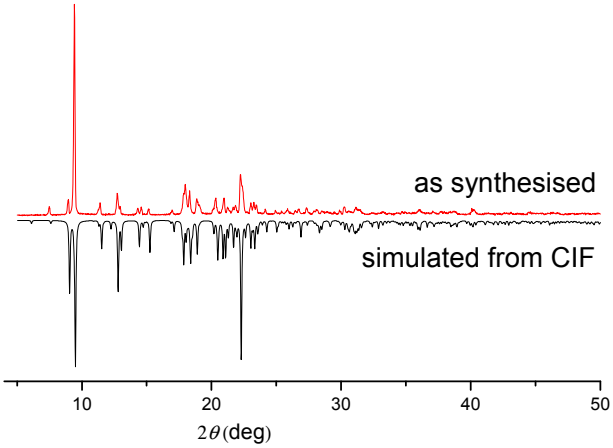

Fig. S14 Simulated and measured powder XRD patterns of **Ag-BF_4**.

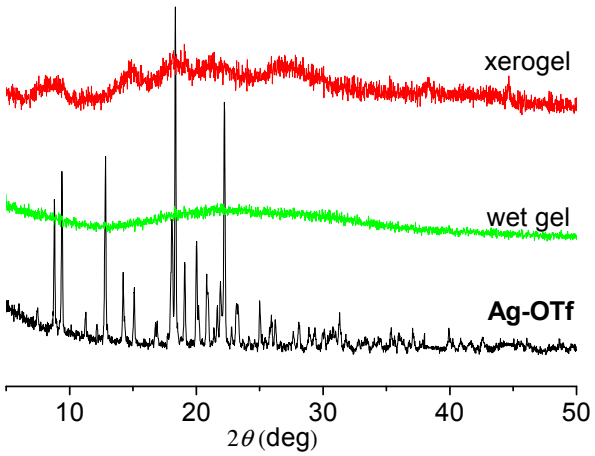

Fig. S15 Measured powder XRD patterns of the AgOTf/L = 1:1 wet gel, the xerogel and **Ag-OTf**.

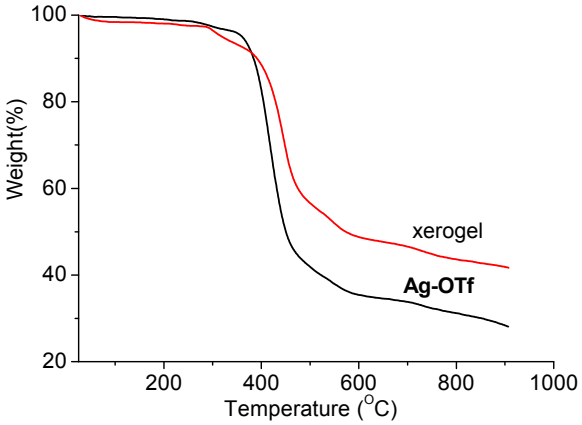

Fig. S16 TGA curves of the AgOTf/L = 1:1 xerogel and **Ag-OTf**.

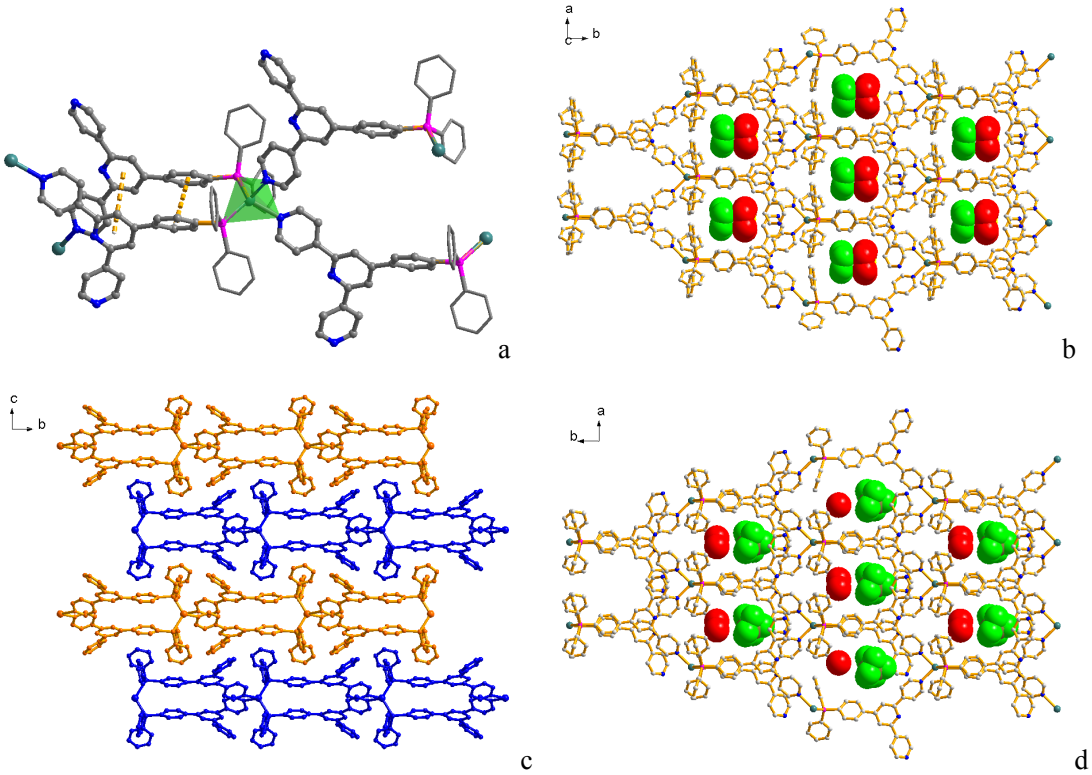

Fig. S17 X-ray structures, a) intralayer π-π interactions, b) OTf^- anions residing in the (4,4) grid cavities, c) the (4,4) networks packing in a ABAB pattern of **Ag-OTf**, and d) BF_4^- anions and solvated water residing in the (4,4) grid cavities of **Ag-BF_4**.

Table S3. Selected bond lengths (Å) and angles (°) for **Ag-OTf** and **Ag-BF_4**.

Ag-OTf		**Ag-BF_4**	
Ag1—N1^{i}	2.3870(19)	Ag1—N1^{i}	2.411(3)
Ag1—N1^{ii}	2.3870(19)	Ag1—N1^{ii}	2.411(3)
Ag1—P1	2.4667(6)	Ag1—P1	2.4866(9)
Ag1—P1^{iii}	2.4667(6)	Ag1—P1^{iii}	2.4866(9)
N1^{i}—Ag1—N1^{ii}	90.47(10)	N1^{i}—Ag1—N1^{ii}	88.77(16)
N1^{i}—Ag1—P1	111.11(5)	N1^{i}—Ag1—P1^{iii}	112.76(9)
N1^{ii}—Ag1—P1	111.72(5)	N1^{ii}—Ag1—P1	112.76(9)
N1^{i}—Ag1—P1^{iii}	111.72(5)	N1^{i}—Ag1—P1	109.89(8)
N1^{ii}—Ag1—P1^{iii}	111.11(5)	N1^{ii}—Ag1—P1^{iii}	109.89(8)
P1—Ag1—P1^{iii}	117.53(3)	P1—Ag1—P1^{iii}	118.85(4)

Symmetry codes for **Ag-BF_4**: (i) -0.5+x, -0.5+y, z; (ii) 1.5-x, -0.5+y, 1.5-z; (iii) 1-x, y, 1.5-z. Symmetry codes for **Ag-OTf**: (i) 2.5-x, 0.5+y, 1.5-z; (ii) -0.5+x, 0.5+y, z; (iii) 2-x, y, 1.5-z.